Journal of Ship Research, Vol. 53, No. 1, March 2009, pp. 19–30

Parametric Identification of Ship Maneuvering Models by Using Support Vector Machines

W. L. Luo* and **Z. J. Zou**†

**School of Naval Architecture, Ocean and Civil Engineering, Shanghai Jiao Tong University, Shanghai, China*
†*State Key Laboratory of Ocean Engineering, Shanghai Jiao Tong University, Shanghai, China*

System identification combined with free-running model tests or full-scale trials is one of the effective methods to determine the hydrodynamic coefficients in the mathematical models of ship maneuvering motion. By analyzing the available data, including rudder angle, surge speed, sway speed, yaw rate, and so forth, a method based on support vector machines (SVM) to estimate the hydrodynamic coefficients is proposed for conventional surface ships. The coefficients are contained in the expansion of the inner product of a linear kernel function. Predictions of maneuvering motion are conducted by using the parameters identified. The results of identification and simulation demonstrate the validity of the identification algorithm proposed. The simultaneous drift and multicollinearity are diminished by introducing an additional ramp signal to the training samples. Comparison between the simulated and predicted motion variables from different maneuvers shows good predictive ability of the trained SVM.

Keywords: maneuvering; hydrodynamics (general); ship motions

1. Introduction

SHIP MANEUVERABILITY is one of the most important hydrodynamic performances and vital to safe navigation. More and more attention has been paid to it especially since the International Maritime Organization (IMO) promulgated the Interim Standards for Ship Manoeuvrability in 1993 (IMO 1993) and the Standards for Ship Manoeuvrability in 2002 (IMO 2002). In these standards, prediction of maneuverability in the stage of ship design is explicitly emphasized.

Mathematical modeling of ship maneuvering motion characterizes the ship dynamic behaviors. Computer simulation based on a mathematical model provides an effective and practical way to evaluate ship maneuverability and controllability in the stage of ship design. To apply this method, it is indispensable to construct and make use of an appropriate mathematical model of ship maneuvering motion. The accuracy of the mathematical model is largely dependent on the accuracy of the hydrodynamic coefficients in it.

Manuscript received at SNAME headquarters June 22, 2007; revised manuscript received April 8, 2008.

Usually, four kinds of methods are available for determining the hydrodynamic coefficients in the ship maneuvering models (ITTC 2005). The first one is based on the captive model tests and is regarded as the most reliable one. The second method, probably the most practical and convenient one, is to use empirical formulas or database. The third method refers to the theoretical or numerical calculation method; the computational fluid dynamics (CFD) technique seems to be a charming and promising approach to determine the hydrodynamic coefficients. The fourth method is system identification (SI) based on full-scale trials or free-running model tests. To apply this method, standard maneuvers are conducted to obtain system inputs (rudder angle, propeller revolution, etc.) and outputs (ship velocities, heading, yaw rate, etc.). Given the input-output data, hydrodynamic coefficients can be determined by using system identification techniques. Since this method can be applied directly to full-scale trials, the so-called scale effects due to different Reynolds numbers between that of the ship model and full-scale ship can be avoided. Several other merits are also mentioned with respect to SI (Haddara & Wang 1999).

In parameter identification techniques, some conventional techniques, such as the model reference method (Hayes 1971), the extended Kalman filter method (Hwang 1980, Abkowitz 1980),

the maximum likelihood method (Åström & Källström 1976), and the recursive prediction error method (Zhou 1989, Källström & Åström 1981), have been proposed to estimate the hydrodynamic coefficients. Least square (LS) estimation or the advanced LS method (Rhee et al. 1998) is also a usual method. However, some problems may exist in these methods, such as sensitivity to the initial values of estimated variables, ill-condition solutions, simultaneous drift of parameters due to dynamic cancellation, and multicollinearity of regressive parameters. In particular, how to eliminate the simultaneous drift and multicollinearity is a difficult problem to be solved. According to the strip theory and slender body theory, viscous forces and moments approximately cancel each other; the inertial forces and moments are balanced by rudder force and moment (Hwang 1982). Hence, the simultaneous drift of hydrodynamic coefficients are inevitable by using step iterative identification, although some measures were proposed to diminish this effect, such as parallel processing, exaggerated over- and underestimation, parameter transformation (Hwang 1982), estimation before modeling (Yoon & Rhee 2003), and modification of input scenario (Yeon et al. 2006). The situation is more severe for nonlinear hydrodynamic coefficients. To avoid the lengthy iterative computation and to diminish cancellation effect, two approaches to estimate the hydrodynamic coefficients have been proposed recently. One involves using Fourier transformation and spectral density functions in the low-frequency domain (Selvam et al. 2005, Bhattacharyya & Haddara 2006). The other is based on neural networks, an artificial intelligence technique (Haddara & Wang 1999, Mahfouz & Haddara 2003). Both methods provide powerful tools to determine hydrodynamic coefficients and to predict ship maneuvering motion. In particular, the latter presents an interesting way to study ship maneuverability. Applying back-propagation neural networks and multiple regression analysis, Haddara and Wang (1999) obtained the nonlinear hydrodynamic coefficients in the Abkowitz model for a surface ship; Mahfouz and Haddara (2003) identified the hydrodynamic coefficients in the equations of coupled heave and pitch motions for an underwater robot. In the present study, another kind of artificial intelligence technique, support vector machines (SVM), is applied to identify the hydrodynamic coefficients.

SVM, as a new technique of artificial intelligence, was put forward in the early 1990s. It is a type of optimized model in which prediction error and model complexity can be simultaneously minimized (Vapnik 1998). It has found wide application in system engineering during the last decade and is considered to be a useful method in system identification (Drezet & Harrison 1998, Gretton et al. 2001, Goethals et al. 2005). It has several outstanding advantages over neural networks. First, the SVM algorithm is based on the criteria of structural risk minimization (SRM). It requires that the error rate on an independent test set be bounded by the sum of the training error rate and a term that depends on the Vapnik-Chervonenkis (VC) dimension of the learning machine. Therefore, high generalization performance can be achieved (Blanz et al. 1996). While the neural networks method is based on the criteria of empirical risk minimization (ERM), which requires only minimization of the training error rate, it has the problem of overlearning for untrained samples. Second, SVM adopts convex quadratic programming, which guarantees a globally optimal solution. On the contrary, the solution of neural networks is apt to plunge into the local optimization. Finally, the problem of the dimensionality curse is easily solved by introduction of a kernel in SVM. This problem is difficult to solve using neural networks.

This paper makes an effort to apply SVM to identify the hydrodynamic coefficients in the mathematical model of ship maneuvering motion in time domain. The training samples are obtained from a simulation program. The nonlinear maneuvering models are approximated by SVM regression models, in which a linear kernel function is adopted. All linear and nonlinear hydrodynamic coefficients are obtained directly from the structure of SVM. It is a batch algorithm and requires no initial estimation of parameters. A ramp signal is designed and added to the training samples to diminish the simultaneous drift and multicollinearity of regressive parameters, and correlation analysis is conducted. Akaike's information criterion (AIC) is applied to analyze the rationality of the modified samples. Finally, predictive ability of the trained SVM is verified by using the simulation results of a 20/20 deg zigzag maneuver to predict other maneuvers.

2. Mathematical model of ship motion

Two kinds of mathematical models were proposed in analyzing ship maneuverability and controllability. The first one is the hydrodynamic model, including the whole model named after Professer Abkowitz (Abkowitz 1964) and the modular model or the MMG model proposed by the Japanese Mathematical Modeling Group. These two models contain many linear and nonlinear hydrodynamic derivatives and/or interaction coefficients. The second class of mathematical model is the response model named after Professor Nomoto. This model contains only simple parameters, such as K, T indices, which can be expressed by the linear hydrodynamic derivatives. The response model has wide application in ship control. From the viewpoint of maneuverability prediction, the hydrodynamic model is preferable. In this paper, we focus on the Abkowitz model in order to verify whether the proposed artificial intelligence technique, SVM, can identify successfully the hydrodynamic coefficients even in such a complicated nonlinear model.

Generally, the maneuvering motion of a surface vessel can be described by motion in surge, sway, and yaw:

$$\begin{aligned}(m - X_{\dot{u}})\dot{u} &= f_1(u, v, r, \delta)\\ (m - Y_{\dot{v}})\dot{v} + (mx_G - Y_{\dot{r}})\dot{r} &= f_2(u, v, r, \delta)\\ (mx_G - N_{\dot{v}})\dot{v} + (I_z - N_{\dot{r}})\dot{r} &= f_3(u, v, r, \delta)\end{aligned} \tag{1}$$

where u, v, r denote the surge speed, sway speed, and yaw rate, respectively, in the body-fixed coordinate system; δ is the rudder angle; m is the mass of the ship; I_z is the inertia moment about the z axis (vertically downward); x_G is the x coordinate of the ship's center of gravity; $X_{\dot{u}}$ et al. are the acceleration derivatives.

The motion variables in equations (1) are expressed as

$$u = u_0 + \Delta u, v = v_0 + \Delta v, r = r_0 + \Delta r, \delta = \delta_0 + \Delta\delta$$

$$U = \sqrt{u^2 + v^2} = \sqrt{(u_0 + \Delta u)^2 + \Delta v^2}$$

where Δu, Δv, Δr, and $\Delta\delta$ are small perturbations from nominal variables u_0, v_0, r_0, and δ_0; U is the ship speed. If the state of straight running is taken as the nominal state, $v_0 = 0$, $r_0 = 0$ holds and $u_0 =$ constant. With nondimensional variables and hydrodynamic coefficients using a prime system, the dynamic equations of motion are given as (Fossen 1994)

$$\begin{bmatrix} m' - X'_{\dot{u}} & 0 & 0 \\ 0 & m' - Y'_{\dot{v}} & m'x'_G - Y'_{\dot{r}} \\ 0 & m'x'_G - N'_{\dot{v}} & I'_z - N'_{\dot{r}} \end{bmatrix} \begin{bmatrix} \Delta\dot{u}' \\ \Delta\dot{v}' \\ \Delta\dot{r}' \end{bmatrix} = \begin{bmatrix} \Delta f'_1 \\ \Delta f'_2 \\ \Delta f'_3 \end{bmatrix} \tag{2}$$

where the nondimensional variables are defined as

$$\Delta u' = \frac{\Delta u}{U}, \Delta v' = \frac{\Delta v}{U}, \Delta r' = \frac{L\Delta r}{U}$$
$$\Delta\dot{u}' = \frac{\Delta\dot{u}}{(U^2/L)}, \Delta\dot{v}' = \frac{\Delta\dot{v}}{(U^2/L)}, \Delta\dot{r}' = \frac{\Delta\dot{r}}{(U^2/L^2)}$$

where L is the ship length; the nondimensional hydrodynamic forces are given in Taylor series expansion as

$$\begin{aligned}
\Delta f'_1 =& X'_u\Delta u' + X'_{uu}\Delta u'^2 + X'_{uuu}\Delta u'^3 + X'_{vv}\Delta v'^2 + X'_{rr}\Delta r'^2 \\
&+ X'_{\delta\delta}\Delta\delta'^2 + X'_{\delta\delta u}\Delta\delta'^2\Delta u' + X'_{vr}\Delta v'\Delta r' + X'_{v\delta}\Delta v'\Delta\delta' \\
&+ X'_{v\delta u}\Delta v'\Delta\delta'\Delta u' + X'_{uvv}\Delta u'\Delta v'^2 + X'_{urr}\Delta u'\Delta r'^2 \\
&+ X'_{uvr}\Delta u'\Delta v'\Delta r' + X'_{r\delta}\Delta r'\Delta\delta' + X'_{ur\delta}\Delta u'\Delta r'\Delta\delta' + X'_0 \\
\Delta f'_2 =& Y'_{0u}\Delta u' + Y'_{0uu}\Delta u'^2 + Y'_v\Delta v' + Y'_r\Delta r' + Y'_\delta\Delta\delta' + Y'_{vvv}\Delta v'^3 \\
&+ Y'_{\delta\delta\delta}\Delta\delta'^3 + Y'_{vvr}\Delta v'^2\Delta r' + Y'_{vv\delta}\Delta v'^2\Delta\delta' + Y'_{v\delta\delta}\Delta v'\Delta\delta'^2 \\
&+ Y'_{\delta u}\Delta\delta'\Delta u' + Y'_{vu}\Delta v'\Delta u' + Y'_{ru}\Delta r'\Delta u' + Y'_{\delta uu}\Delta\delta'\Delta u'^2 \\
&+ Y'_{rrr}\Delta r'^3 + Y'_{vrr}\Delta v'\Delta r'^2 + Y'_{vuu}\Delta v'\Delta u'^2 + Y'_{ruu}\Delta r'\Delta u'^2 \\
&+ Y'_{r\delta\delta}\Delta r'\Delta\delta'^2 + Y'_{rr\delta}\Delta r'^2\Delta\delta' + Y'_{rv\delta}\Delta r'\Delta v'\Delta\delta' + Y'_0 \\
\Delta f'_3 =& N'_{0u}\Delta u' + N'_{0uu}\Delta u'^2 + N'_v\Delta v' + N'_r\Delta r' + N'_\delta\Delta\delta' + N'_{vvv}\Delta v'^3 \\
&+ N'_{\delta\delta\delta}\Delta\delta'^3 + N'_{vvr}\Delta v'^2\Delta r' + N'_{vv\delta}\Delta v'^2\Delta\delta' + N'_{v\delta\delta}\Delta v'\Delta\delta'^2 \\
&+ N'_{\delta u}\Delta\delta'\Delta u' + N'_{vu}\Delta v'\Delta u' + N'_{ru}\Delta r'\Delta u' + N'_{\delta uu}\Delta\delta'\Delta u'^2 \\
&+ N'_{rrr}\Delta r'^3 + N'_{vrr}\Delta v'\Delta r'^2 + N'_{vuu}\Delta v'\Delta u'^2 + N'_{ruu}\Delta r'\Delta u'^2 \\
&+ N'_{r\delta\delta}\Delta r'\Delta\delta'^2 + N'_{rr\delta}\Delta r'^2\Delta\delta' + N'_{rv\delta}\Delta r'\Delta v'\Delta\delta' + N'_0
\end{aligned} \tag{3}$$

For the purpose of parametric identification and computer simulation, the nondimensional form of equations (2) is rewritten as

$$\begin{aligned}
\Delta\dot{u}' =& \Delta f'_1/(m' - X'_{\dot{u}}) \\
\Delta\dot{v}' =& \left[(I'_z - N'_{\dot{r}})\Delta f'_2 - (m'x'_G - Y'_{\dot{r}})\Delta f'_3\right]/S \\
\Delta\dot{r}' =& \left[(m' - Y'_{\dot{v}})\Delta f'_3 - (m'x'_G - N'_{\dot{v}})\Delta f'_2\right]/S
\end{aligned} \tag{4}$$

where $S = (I'_z - N'_{\dot{r}})(m' - Y'_{\dot{v}}) - (m'x'_G - Y'_{\dot{r}})(m'x'_G - N'_{\dot{v}})$.

There are one acceleration derivative and 15 velocity derivatives in the surge equation, two acceleration derivatives and 21 velocity derivatives in the sway and yaw equation, respectively. Moreover, two bias forces and one bias moment (X'_0, Y'_0, N'_0) are contained in the three equations. In this parametric system, five acceleration derivatives are assumed known, whereas the other 60 parameters are to be identified.

3. Support vector regression

Derived from the statistical learning theory, the support vector machines (SVM) method was applied in the area of pattern recognition at the beginning, then was successfully used in function approximation, regression estimation, and signal processing by introducing ε insensitivity (Vapnik 1999). It was considered a universal learning tool (Vapnik 2005). The object of the present study is to obtain the hydrodynamic coefficients from the SVM regression model.

SVM for regression purposes has a general approximation function form for a multi-input/single-output (MISO) system:

$$y = \boldsymbol{w}^{\mathrm{T}} \cdot \Phi(\boldsymbol{x}) + b \tag{5}$$

where y is the scalar output of the system; $\boldsymbol{x}$ is the input vector of the system; $\boldsymbol{w}$ is a weight matrix; b is a constant; $\boldsymbol{w} \in R^n$, $b \in R$; R^n is the n-dimensional real space. With the help of a nonlinear function $\Phi(\cdot)$, a linear function is constructed in a so-called high-dimensional feature space to approximate the hidden mapping contained in the original training samples $(\boldsymbol{x}_i, y_i)(i = 1, 2, \cdots l)$ $(\boldsymbol{x}_i \in R^n, y_i \in R)$. l is the number of samples.

Based on SRM, a cost function in standard SVM is defined as

$$\min_{\mathbf{w},b,\xi}\left\{\frac{1}{2}\boldsymbol{w}^{\mathrm{T}}\boldsymbol{w} + C\sum_{i=1}^{l}(\xi_i + \xi_i^*)\right\} \tag{6}$$

subject to

$$\left.\begin{aligned} y_i - [\boldsymbol{w}^{\mathrm{T}}\Phi(\boldsymbol{x}_i) + b] \le \varepsilon + \xi_i \\ \boldsymbol{w}^{\mathrm{T}}\Phi(\boldsymbol{x}_i) + b - y_i \le \varepsilon + \xi_i^* \\ \xi_i, \xi_i^* \ge 0 \end{aligned}\right\} \tag{7}$$

where the ε insensitivity means the accuracy of regression. The slack variables ξ_i and ξ_i^* are introduced to guarantee the existence of the solution of the cost function when regression errors exceed the bound of ε. Note that the first term in expression (6) implies the minimization of the VC dimension, reflecting the generalization ability of the learning machine. The second term, accompanied by the so-called regularization parameter C, which is positive, is designed to control the tradeoff between empirical error and complexity of the model. Then a Lagrangian function is constructed. It is composed of expression (6) and an equality constraint derived from the inequalities (7), multiplied by Lagrangian factors. Applying convex quadratic programming and the Kuhn-Tucker theorem, the Lagrangian factors and bias b can be calculated. By introducing a kernel function, the object function can be approximated by the linear combination of Lagrangian factors, the kernel function, and b (Vapnik 1998).

In standard SVM, the parameters ε and C are very important factors while constructing SVM. However, how to properly choose these two parameters remains unsolved and these are usually found from numerical experiments. For example, a larger C usually improves the accuracy of regression but degrades the generalization ability, because the weight of the VC dimension decreases. On the other hand, a smaller C may increase the

learning errors and consequently make its generalization ability better. This contradictive issue also occurs while selecting ε. To avoid the uncertainties in selecting structural parameters, some improvements have been made, such as v-SVM (Schölkopf et al. 2000), least squares (LS)-SVM (Suykens & Vandewalle 1999), and w-SVM (Lin & Wang 2002). Among these modified algorithms, LS-SVM is an effective and simple one. It converts the convex quadratic programming in standard SVM to solving a linear matrix equation. The constraint conditions are fewer and simpler than those in standard SVM.

LS-SVM adopts a quadratic term in the cost function

$$\min_{\mathbf{w},b,\xi}\left\{\frac{1}{2}\boldsymbol{w}^{\mathrm{T}}\boldsymbol{w}+\frac{1}{2}C\sum_{i=1}^{l}\xi_i^2\right\} \tag{8}$$

subject to

$$y_i-[\boldsymbol{w}^{\mathrm{T}}\boldsymbol{\Phi}(\boldsymbol{x}_i)+b]=\xi_i \tag{9}$$

The Lagrangian function is formulated as

$$\begin{aligned}\mathbf{L}(\boldsymbol{w},b,\xi,\alpha)=&\frac{1}{2}\boldsymbol{w}^{\mathrm{T}}\boldsymbol{w}+\frac{1}{2}C\sum_{i=1}^{l}\xi_i^2\\&-\sum_{i=1}^{l}\alpha_i[\xi_i-y_i+\boldsymbol{w}^{\mathrm{T}}\boldsymbol{\Phi}(\boldsymbol{x}_i)+b]\end{aligned} \tag{10}$$

where α_i is a Lagrangian factor. The optimal conditions are

$$\boldsymbol{w}=\sum_{i=1}^{l}\alpha_i\boldsymbol{\Phi}(\boldsymbol{x}_i) \tag{11}$$

$$\sum_{i=1}^{l}\alpha_i=0 \tag{12}$$

$$C\cdot\xi_i=\alpha_i \tag{13}$$

$$\boldsymbol{w}^{\mathrm{T}}\boldsymbol{\Phi}(\boldsymbol{x}_i)+b+\xi_i-y_i=0 \tag{14}$$

Substituting (11) and (13) into (14), the following system of linear equations can be obtained:

$$\begin{bmatrix}0&1&\cdots&1\\1&\boldsymbol{\Phi}^{\mathrm{T}}(\boldsymbol{x}_1)\boldsymbol{\Phi}(\boldsymbol{x}_1)+\frac{1}{C}&\cdots&\boldsymbol{\Phi}^{\mathrm{T}}(\boldsymbol{x}_1)\boldsymbol{\Phi}(\boldsymbol{x}_l)\\\vdots&\vdots&\ddots&\vdots\\1&\boldsymbol{\Phi}^{\mathrm{T}}(\boldsymbol{x}_l)\boldsymbol{\Phi}(\boldsymbol{x}_1)&\cdots&\boldsymbol{\Phi}^{\mathrm{T}}(\boldsymbol{x}_l)\boldsymbol{\Phi}(\boldsymbol{x}_l)+\frac{1}{C}\end{bmatrix}\begin{bmatrix}b\\\alpha_1\\\vdots\\\alpha_l\end{bmatrix}=\begin{bmatrix}0\\y_1\\\vdots\\y_l\end{bmatrix} \tag{15}$$

To simplify the calculation and to avoid the so-called dimensionality curse in the "virtual" high-dimensional space, kernel functions are introduced. Generally, the basic formulation of kernel function can be expressed as a form of inner product $K(\boldsymbol{x}_i,\boldsymbol{x}_j)=[\boldsymbol{\Phi}(\boldsymbol{x}_i)\cdot\boldsymbol{\Phi}(\boldsymbol{x}_j)]$ and it should satisfy the Mercer condition. Consequently, the efficiency of SVM relies on the capacity of a training sample set rather than its dimension. Once the parameters b and α_i are calculated, the function to be approximated is determined by

$$y=\sum_{i=1}^{n}\alpha_iK(\boldsymbol{x}_i,\boldsymbol{x})+b \tag{16}$$

where n denotes the number of the so-called support vectors with respect to nonzero α_i.

For a MIMO system, the matrix equation is given as

$$\begin{bmatrix}0&1&\cdots&1\\1&\boldsymbol{\Phi}^{\mathrm{T}}(\boldsymbol{x}_1)\boldsymbol{\Phi}(\boldsymbol{x}_1)+\frac{1}{C}&\cdots&\boldsymbol{\Phi}^{\mathrm{T}}(\boldsymbol{x}_1)\boldsymbol{\Phi}(\boldsymbol{x}_l)\\\vdots&\vdots&\ddots&\vdots\\1&\boldsymbol{\Phi}^{\mathrm{T}}(\boldsymbol{x}_l)\boldsymbol{\Phi}(\boldsymbol{x}_1)&\cdots&\boldsymbol{\Phi}^{\mathrm{T}}(\boldsymbol{x}_l)\boldsymbol{\Phi}(\boldsymbol{x}_l)+\frac{1}{C}\end{bmatrix}\begin{bmatrix}b_1&b_2&\cdots&b_k\\\alpha_{11}&\alpha_{21}&\cdots&\alpha_{k1}\\\vdots&\vdots&\ddots&\vdots\\\alpha_{1l}&\alpha_{2l}&\cdots&\alpha_{kl}\end{bmatrix}=\begin{bmatrix}0&0&\cdots&0\\y_{11}&y_{21}&\cdots&y_{k1}\\\vdots&\vdots&\ddots&\vdots\\y_{1l}&y_{2l}&\cdots&y_{kl}\end{bmatrix} \tag{17}$$

4. Identification and prediction

4.1. Reconstruction of ship maneuvering model

SVM is used to approximate the nonlinear functions $\Delta f_i'(i=1,2,3)$ in equations (3) and identify the hydrodynamic coefficients. First of all, in order to apply computer simulation, discretizing the continuous equation of motion is necessary. Given a proper sampling interval h, the differential variables of motion can be expressed by using Euler's stepping method as

$$\begin{aligned}\Delta\dot{u}&=[\Delta u(k+1)-\Delta u(k)]/h\\\Delta\dot{v}&=[\Delta v(k+1)-\Delta v(k)]/h\\\Delta\dot{r}&=[\Delta r(k+1)-\Delta r(k)]/h\end{aligned}$$

where k and $k+1$ are the indices for two successive sampling times. For convenience of simulation, the nondimensional variables $\Delta u'$, $\Delta v'$, $\Delta r'$ are reverted to their original dimensional forms. Three discrete motion equations are obtained:

$$\begin{aligned}\Delta u(k+1)=&\Delta u(k)+\frac{h}{L(m'-X_{\dot{u}}')}[X_u'\Delta u(k)U(k)\\&+X_{uu}'\Delta u^2(k)+X_{uuu}'\Delta u^3(k)/U(k)\\&+X_{vv}'\Delta v^2(k)+X_{rr}'\Delta r^2(k)L^2+X_{\delta\delta}'\Delta\delta^2(k)U^2(k)\\&+X_{\delta\delta u}'\Delta\delta^2(k)\Delta u(k)U(k)+X_{vr}'\Delta v(k)\Delta r(k)L\\&+X_{v\delta}'\Delta v(k)\Delta\delta(k)U(k)+X_{v\delta u}'\Delta v(k)\Delta\delta(k)\Delta u(k)\\&+X_{uvv}'\Delta u(k)\Delta v^2(k)/U(k)+X_{urr}'\Delta u(k)\Delta r^2(k)L^2/U(k)\\&+X_{uvr}'\Delta u(k)\Delta v(k)\Delta r(k)L/U(k)+X_{r\delta}'\Delta r(k)\Delta\delta(k)LU(k)\\&+X_{ur\delta}'\Delta u(k)\Delta r(k)\Delta\delta(k)L+X_0'U^2(k)]\end{aligned}$$

$$\begin{aligned}\Delta v(k+1)=&\Delta v(k)+\frac{h(I_z'-N_{\dot{r}}')}{SL}[Y_0'U^2(k)+Y_{0u}'\Delta u(k)U(k)\\&+Y_{0uu}'\Delta u^2(k)+Y_v'\Delta v(k)U(k)+Y_r'\Delta r(k)U(k)L\\&+Y_\delta'\Delta\delta(k)U^2(k)+Y_{vvv}'\Delta v^3(k)/U(k)+Y_{\delta\delta\delta}'\Delta\delta^3U^2(k)\\&+Y_{vvr}'\Delta v^2(k)\Delta r(k)L/U(k)+Y_{vv\delta}'\Delta v^2(k)\Delta\delta(k)\\&+Y_{v\delta\delta}'\Delta v(k)\Delta\delta^2(k)U(k)+Y_{\delta u}'\Delta\delta(k)\Delta u(k)U(k)\\&+Y_{vu}'\Delta v(k)\Delta u(k)+Y_{ru}'\Delta r(k)\Delta u(k)L+Y_{\delta uu}'\Delta\delta(k)\Delta u^2(k)\\&+Y_{rrr}'\Delta r^3(k)L^3/U(k)+Y_{vrr}'\Delta v(k)\Delta r^2(k)L^2/U(k)\\&+Y_{vuu}'\Delta v(k)\Delta u^2(k)/U(k)+Y_{ruu}'\Delta r(k)\Delta u^2(k)L/U(k)\\&+Y_{r\delta\delta}'\Delta r(k)\Delta\delta^2(k)LU(k)+Y_{rr\delta}'\Delta r^2(k)\Delta\delta(k)L^2\end{aligned}$$

$$
\begin{aligned}
&+Y'_{rv\delta}\Delta r(k)\Delta v(k)\Delta\delta(k)L]-\frac{h(m'x'_G-Y'_{\dot r})}{SL}[N'_0U^2(k)\\
&+N'_{0u}\Delta u(k)U(k)+N'_{0uu}\Delta u^2(k)+N'_v\Delta v(k)U(k)\\
&+N'_r\Delta r(k)U(k)L+N'_\delta\Delta\delta(k)U^2(k)+N'_{vvv}\Delta v^3(k)/U(k)\\
&+N'_{\delta\delta\delta}\Delta\delta^3(k)U^2(k)+N'_{vvr}\Delta v^2(k)\Delta r(k)L/U(k)\\
&+N'_{vv\delta}\Delta v^2(k)\Delta\delta(k)+N'_{v\delta\delta}\Delta v(k)\Delta\delta^2(k)U(k)\\
&+N'_{\delta u}\Delta\delta(k)\Delta u(k)U(k)+N'_{vu}\Delta v(k)\Delta u(k)\\
&+N'_{ru}\Delta r(k)\Delta u(k)L+N'_{\delta uu}\Delta\delta(k)\Delta u^2(k)\\
&+N'_{rrr}\Delta r^3(k)L^3/U(k)+N'_{vrr}\Delta v(k)\Delta r^2(k)L^2/U(k)\\
&+N'_{vuu}\Delta v(k)\Delta u^2(k)/U(k)+N'_{ruu}\Delta r(k)\Delta u^2(k)L/U(k)\\
&+N'_{r\delta\delta}\Delta r(k)\Delta\delta^2(k)LU(k)+N'_{rr\delta}\Delta r^2(k)\Delta\delta(k)L^2\\
&+N'_{rv\delta}\Delta r(k)\Delta v(k)\Delta\delta(k)L]
\end{aligned}
$$

$$
\begin{aligned}
\Delta r(k+1)=&\Delta r(k)-\frac{h(m'x'_G-N'_{\dot v})}{SL^2}[Y'_0U^2(k)+Y'_{0u}\Delta u(k)U(k)\\
&+Y'_{0uu}\Delta u^2(k)+Y'_v\Delta v(k)U(k)+Y'_r\Delta r(k)U(k)L\\
&+Y'_\delta\Delta\delta(k)U^2(k)+Y'_{vvv}\Delta v^3(k)/U(k)+Y'_{\delta\delta\delta}\Delta\delta^3U^2(k)\\
&+Y'_{vvr}\Delta v^2(k)\Delta r(k)L/U(k)+Y'_{vv\delta}\Delta v^2(k)\Delta\delta(k)\\
&+Y'_{v\delta\delta}\Delta v(k)\Delta\delta^2(k)U(k)+Y'_{\delta u}\Delta\delta(k)\Delta u(k)U(k)\\
&+Y'_{vu}\Delta v(k)\Delta u(k)+Y'_{ru}\Delta r(k)\Delta u(k)L+Y'_{\delta uu}\Delta\delta(k)\Delta u^2(k)\\
&+Y'_{rrr}\Delta r^3(k)L^3/U(k)+Y'_{vrr}\Delta v(k)\Delta r^2(k)L^2/U(k)\\
&+Y'_{vuu}\Delta v(k)\Delta u^2(k)/U(k)+Y'_{ruu}\Delta r(k)\Delta u^2(k)L/U(k)\\
&+Y'_{r\delta\delta}\Delta r(k)\Delta\delta^2(k)LU(k)+Y'_{rr\delta}\Delta r^2(k)\Delta\delta(k)L^2\\
&+Y'_{rv\delta}\Delta r(k)\Delta v(k)\Delta\delta(k)L]+\frac{h(m'-Y'_{\dot v})}{SL^2}[N'_0U^2(k)\\
&+N'_{0u}\Delta u(k)U(k)+N'_{0uu}\Delta u^2(k)+N'_v\Delta v(k)U(k)\\
&+N'_r\Delta r(k)U(k)L+N'_\delta\Delta\delta(k)U^2(k)+N'_{vvv}\Delta v^3(k)/U(k)\\
&+N'_{\delta\delta\delta}\Delta\delta^3(k)U^2(k)+N'_{vvr}\Delta v^2(k)\Delta r(k)L/U(k)\\
&+N'_{vv\delta}\Delta v^2(k)\Delta\delta(k)+N'_{v\delta\delta}\Delta v(k)\Delta\delta^2(k)U(k)\\
&+N'_{\delta u}\Delta\delta(k)\Delta u(k)U(k)+N'_{vu}\Delta v(k)\Delta u(k)\\
&+N'_{ru}\Delta r(k)\Delta u(k)L+N'_{\delta uu}\Delta\delta(k)\Delta u^2(k)\\
&+N'_{rrr}\Delta r^3(k)L^3/U(k)+N'_{vrr}\Delta v(k)\Delta r^2(k)L^2/U(k)\\
&+N'_{vuu}\Delta v(k)\Delta u^2(k)/U(k)+N'_{ruu}\Delta r(k)\Delta u^2(k)L/U(k)\\
&+N'_{r\delta\delta}\Delta r(k)\Delta\delta^2(k)LU(k)+N'_{rr\delta}\Delta r^2(k)\Delta\delta(k)L^2\\
&+N'_{rv\delta}\Delta r(k)\Delta v(k)\Delta\delta(k)L] \qquad (18)
\end{aligned}
$$

Introducing new symbols, equations (18) can be rewritten as

$$
\begin{aligned}
\Delta u(k+1)&=\boldsymbol{AX}\\
\Delta v(k+1)&=\boldsymbol{BY}\\
\Delta r(k+1)&=\boldsymbol{CZ}
\end{aligned} \qquad (19)
$$

where the variable vector and coefficient vector are given as

$$
\begin{aligned}
\boldsymbol{X}=&[\Delta u(k),\Delta u(k)U(k),\Delta u^2(k),\Delta u^3(k)/U(k),\Delta v^2(k),\\
&\Delta r^2(k),\Delta\delta^2(k)U^2(k),\Delta\delta^2(k)\Delta u(k)U(k),\Delta v(k)\Delta r(k),\\
&\Delta v(k)\Delta\delta(k)U(k),\Delta v(k)\Delta\delta(k)\Delta u(k),\Delta u(k)\Delta v^2(k)/U(k),\\
&\Delta u(k)\Delta r^2(k)/U(k),\Delta u(k)\Delta v(k)\Delta r(k)/U(k),\\
&\Delta r(k)\Delta\delta(k)U(k),\Delta u(k)\Delta r(k)\Delta\delta(k),U^2(k)]^{\mathrm{T}}_{17\times1}\\
\boldsymbol{Y}=&[\Delta v(k),U^2(k),\Delta u(k)U(k),\Delta u^2(k),\Delta v(k)U(k),\\
&\Delta r(k)U(k),\Delta\delta(k)U^2(k),\Delta v^3(k)/U(k),\Delta\delta^3U^2(k),\\
&\Delta v^2(k)\Delta r(k)/U(k),\Delta v^2(k)\Delta\delta(k),\Delta v(k)\Delta\delta^2(k)U(k),\\
&\Delta\delta(k)\Delta u(k)U(k),\Delta v(k)\Delta u(k),\Delta r(k)\Delta u(k),\\
&\Delta\delta(k)\Delta u^2(k),\Delta r^3(k)/U(k),\Delta v(k)\Delta r^2(k)/U(k),\\
&\Delta v(k)\Delta u^2(k)/U(k),\Delta r(k)\Delta u^2(k)/U(k),\Delta r(k)\Delta\delta^2(k)U(k),\\
&\Delta r^2(k)\Delta\delta(k),\Delta r(k)\Delta v(k)\Delta\delta(k)]^{\mathrm{T}}_{23\times1}\\
\boldsymbol{Z}=&[\Delta r(k),U^2(k),\Delta u(k)U(k),\Delta u^2(k),\Delta v(k)U(k),\Delta r(k)U(k),\\
&\Delta\delta(k)U^2(k),\Delta v^3(k)/U(k),\Delta\delta^3U^2(k),\Delta v^2(k)\Delta r(k)/U(k),\\
&\Delta v^2(k)\Delta\delta(k),\Delta v(k)\Delta\delta^2(k)U(k),\Delta\delta(k)\Delta u(k)U(k),\\
&\Delta v(k)\Delta u(k),\Delta r(k)\Delta u(k),\Delta\delta(k)\Delta u^2(k),\Delta r^3(k)/U(k),\\
&\Delta v(k)\Delta r^2(k)/U(k),\Delta v(k)\Delta u^2(k)/U(k),\Delta r(k)\Delta u^2(k)/U(k),\\
&\Delta r(k)\Delta\delta^2(k)U(k),\Delta r^2(k)\Delta\delta(k),\Delta r(k)\Delta v(k)\Delta\delta(k)]^{\mathrm{T}}_{23\times1}\\
\boldsymbol{A}=&[1\quad a_1\quad a_2\quad a_3\quad\cdots\quad a_{16}]_{1\times17}\\
\boldsymbol{B}=&[1\quad b_1\quad b_2\quad b_3\quad\cdots\quad b_{22}]_{1\times23}\\
\boldsymbol{C}=&[1\quad c_1\quad c_2\quad c_3\quad\cdots\quad c_{22}]_{1\times23}
\end{aligned} \qquad (20)
$$

The above coefficient vectors can be identified by using SVM. To illustrate the procedure in a simple way, the surge motion is taken as an example:

$$\boldsymbol{x}_i=\boldsymbol{X},y_i=\Delta u(k+1)$$

and the linear kernel $K(\boldsymbol{x}_i,\boldsymbol{x}_j)=(\boldsymbol{x}_i\cdot\boldsymbol{x}_j)$ is selected. The learning result by SVM is

$$y_i=\left(\sum_{j=1}^{n}\alpha_j\boldsymbol{x}_j\right)\cdot\boldsymbol{x}_i+b \qquad (21)$$

Compared with equations (19), if SVM has approximated the object function well, one has

$$\mathbf{A}=\sum_{j=1}^{n}\alpha_j\boldsymbol{x}_j \qquad (22)$$

Similar to the neural networks approach, the SVM algorithm aims to set up a correct mapping of input-output samples. Just like in neural networks, how to express the mapping is a trick in SVM (Vapnik 2005). As can be seen from equations (18), the mapping from inputs $\{\Delta u(k),\Delta v(k),\Delta r(k),\Delta\delta(k),U(k)\}$ to outputs $\Delta u(k+1)$, $\Delta v(k+1)$, and $\Delta r(k+1)$ is nonlinear. Several nonlinear kernel functions, such as the polynomial function $K(\boldsymbol{x},\boldsymbol{x}_i)=[(\boldsymbol{x}\cdot\boldsymbol{x}_i)+d]^p$, the Gaussian function $K(\boldsymbol{x},\boldsymbol{x}_i)=\exp(-\parallel\boldsymbol{x}-\boldsymbol{x}_i\parallel^2/2\sigma^2)$, and the sigmoid function $K(\boldsymbol{x},\boldsymbol{x}_i)=\tanh(\kappa(\boldsymbol{x}\cdot\boldsymbol{x}_i)+\upsilon)$, are often used while approximating nonlinear functions. In the present study, a polynomial kernel function was considered at the beginning, since the parameters a_i, b_i, and c_i could be obtained directly from the polynomial expansion. However, our identification practice showed that picking up the coefficients from the fifth-order polynomial expansion and

calculating the polynomial kernel matrix were difficult and tedious. Fortunately, if the structure of the mathematical model is known beforehand, the linear kernel is preferable to the polynomial one. As mentioned before, the efficiency of SVM mainly depends on sample size and has no relation to the dimension of the input vector. Moreover, equations (18) are linear with respect to the hydrodynamic coefficients. Therefore, ***X, Y, Z*** may be selected as the input of surge, sway, and yaw equations. With a linear kernel, the parameters a_i, b_i, c_i can be easily obtained from the inner product expansion, after the SVM has successfully approximated equations (19). In addition, the solution is unique if the elements in the input vector are linearly independent of each other. Comparing equation (21) with the first row of (19), one has

$$\left(\boldsymbol{A} - \sum_{i=1}^{n} \alpha_i \boldsymbol{x}_i\right) \cdot \boldsymbol{X} = 0 \tag{23}$$

while the bias b in equation (21) should be zero or negligible. If the elements in the vector $\boldsymbol{X}$ are linearly independent of each other, the above algebraic equation (23) has only zero solution, that is,

$$\boldsymbol{A} = \sum_{i=1}^{n} \alpha_i \boldsymbol{x}_i.$$

Similar analysis can be made for the sway and yaw equations.

Obviously, the hydrodynamic coefficients are contained in the parameters a_i, b_i, and c_i identified by SVM. In a discrete surge motion equation, the hydrodynamic velocity derivatives and X'_0 can be easily calculated after the parameter a_i ($i = 1,2,\ldots16$) has been identified. To obtain the hydrodynamic coefficients in a sway and yaw equation, it is necessary to solve a series of combined equations. For example, the hydrodynamic coefficients Y'_0, N'_0 are obtained by solving the following equation:

$$\begin{bmatrix} \dfrac{h(I'_z - N'_{\dot{r}})}{SL} - \dfrac{h(m'x'_G - Y'_{\dot{r}})}{SL} \\ -\dfrac{h(m'x'_G - N'_{\dot{v}})}{SL^2} \dfrac{h(m' - Y'_{\dot{v}})}{SL^2} \end{bmatrix} \begin{bmatrix} Y'_0 \\ N'_0 \end{bmatrix} = \begin{bmatrix} b_1 \\ c_1 \end{bmatrix} \tag{24}$$

The other hydrodynamic coefficients can be obtained in a similar way.

It should be noted that the five acceleration derivatives $X'_{\dot{u}}, Y'_{\dot{v}}, Y'_{\dot{r}}, N'_{\dot{v}}$, and $N'_{\dot{r}}$ contained in a_i, b_i, and c_i are obtained by theoretical calculation or tests rather than by system identification because of parameter identifiability (Abkowitz 1980, Hwang 1982). They are treated as known constants during identification. These derivatives could be identified, provided that the forces acting on the ship and the acceleration could be measured in sea trials or free-running model tests.

4.2. Parametric identification by using LS-SVM

4.2.1. Selection of sample. A *Mariner* class vessel is taken as the object model (Chislett & Strom-Tejsen 1965). Table 1 gives the main particulars of the ship. Note that in the hydrodynamic model, only 10 hydrodynamic coefficients in surge equation, 15 in sway equation, and 15 in yaw equation are taken into account, while the others are zeros.

The training samples are obtained from computer simulation programs by using standard 20/20 deg zigzag maneuvers at an approach speed of 15 knots (7.717 m/s). For every single variable, such as surge speed u, the sampling interval is 0.5 s. Simulation time is 600 s. Hence, a total of 1,201 points are obtained, from which 300 points are drawn out at equal intervals, starting from the initial time. Thus, the interval between two adjoining points is 2 s and the 300 points cover the overall zigzag maneuver. The same operation is conducted on sway speed, yaw rate, rudder angle, and ship velocity, respectively. Then 300 training samples consist of (for surge speed)

$$input: \{\Delta u(k), \Delta v(k), \Delta r(k), \Delta\delta(k), U(k)\} \rightarrow output: \{\Delta u(k+1)\}$$

The same operation is conducted for sway speed and yaw rate. Note that it is better to use a small number of training samples if possible. As pointed out, the LS-SVM usually has no sparse solution, especially for the regression problem (Keerthi & Shevade 2003). Almost every input becomes a support vector, and consequently the convergence rate of the solution slows down dramatically in a large problem. Also, calculation of the kernel matrix dominates the run time in this case. However, a sample that is too small cannot reflect the nature of the object. Some methods were proposed, such as the decomposition method (Laskov 2002), the sequential minimal optimization (Platt 1998, Keerthi & Shevade 2003), and the incremental method (Syed et al. 1999). They mainly dealt with sparse solution of classification, yet few were done with regression using LS-SVM. In the present study, taking the tradeoff between the convergence rate of the algorithm and the accuracy of the regression model into account, the number of samples chosen is 300. Comparisons from 50 samples to 600 samples are shown in Table 2.

It can be seen that a smaller sample results in a bigger estimation error. Taking convergence rate into account, 300 samples are chosen.

4.2.2. Diminishing the simultaneous drift and multicollinearity. A cancellation effect is evitable due to the inherent dynamics of ships, especially in standard maneuvers, such as zigzag or turning. Different excitations, such as a pseudo random binary sequence signal or a modified input scenario, provide an effective way. However, for the available sample, for example, from the zigzag maneuver, a few effective measures were proposed, especially for nonlinear hydrodynamic coefficients. Besides this effect, another problem, the so-called multicollinearity in regression analysis, also exists. If the input variables are strongly linearly dependent

Table 1 Main particulars of *Mariner* class vessel

Parameter	Magnitude
Length overall (L_{oa})	171.8 m
Length between perpendiculars (L_{pp})	160.93 m
Maximum beam (B)	23.17 m
Design draft (T)	8.23 m
Design displacement (∇)	18,541 m^3

Table 2 Standard deviation of parameter error

N	SD (surge)	SD (*sway*)	SD (*yaw*)
50	2.3×10^{-3}	1.2×10^{-3}	6.0×10^{-3}
100	4.2×10^{-4}	6.1×10^{-4}	3.7×10^{-3}
300	3.3×10^{-5}	1.8×10^{-4}	2.6×10^{-4}
600	3.0×10^{-6}	9.1×10^{-5}	3.0×10^{-5}

Note: N denotes the number of samples; SD denotes the standard deviation of parameter error.

on each other, the regression results of their coefficients may be incorrect or worse, even if the predicted outputs agree well with the desired. The case is more possible and serious when the system contains a large number of parameters to be identified. The multicollinearity cannot be eliminated but moderated, because the input variables are always linearly dependent on each other, more or less. Some remedies were proposed to moderate the degree of multicollinearity, such as pruning variables, principal component regression (Massy 1965), partial least squares (Wold et al. 1984), and a group method of data handling (Ivakhnenko & Muller 1995). In ship maneuverability, ridge regression analysis was applied (Yoon & Rhee 2003, Yeon et al. 2006). In the present study, a simple measure is taken to diminish the multicollinearity. Opposite to pruning variables, an additional ramp signal $y(k+1) = y(k) + \lambda$ is designed to reconstruct the samples, synthetically taking the multicollinearity and accuracy of the regression model into account. First, the introduction of an additional signal means that one obtains a new parameter system of the original hydrodynamic model in the linear high-dimensional feature space. This system moderates the multicollinearity, which can be checked by the correlation coefficients. Nevertheless, the parametric expression of the original system remains unchanged. Therefore, the accuracy of parametric estimation is improved. From the viewpoint of diminishing simultaneous drift, the signal can be regarded as an additional excitation. Second, in choosing the constant λ, the AIC, parameter error, and condition number of the coefficient matrix in equation (15) are taken into account, as shown in Tables 3 to 5. The likelihood function in AIC and AIC value are given as

$$\hat{L} = -\frac{N}{2}(1 + \log 2\pi + \log\frac{R^{\mathrm{T}}R}{N}) \tag{25}$$

$$\text{AIC value} = -\frac{2\hat{L}}{N} + \frac{2\kappa}{N} \tag{26}$$

where R is the residual error vector of the regression model, and κ is the number of parameters.

It can be seen that a smaller λ decreases the accuracy of the regression model, whereas increasing λ makes the condition number (CN) of the coefficient matrix larger, which implies the possibility of an ill-condition solution (equation 15 or 17). As a tradeoff, $\lambda = 0.01$ is considered reasonable.

Table 3 Statistics of surge regression models

λ	AIC Value	SD	CN
0.001	−20.6	5.6×10^{-4}	2.2×10^{8}
0.01	−25.3	3.3×10^{-5}	2.2×10^{8}
0.1	−29.2	2.1×10^{-5}	10.0×10^{8}

Table 4 Statistics of sway regression models

λ	AIC value	SD	CN
0.001	−21.0	2.3×10^{-4}	7.0×10^{9}
0.01	−24.8	1.8×10^{-4}	7.0×10^{9}
0.1	−25.4	1.8×10^{-4}	7.6×10^{9}

Table 5 Statistics of yaw regression models

λ	AIC value	SD	CN
0.001	−21.0	5.6×10^{-3}	7.0×10^{9}
0.01	−25.5	2.8×10^{-4}	7.0×10^{9}
0.1	−29.6	2.8×10^{-4}	7.6×10^{9}

4.2.3. Identification and simulation results. Table 6 shows the comparison of the identification results with the original values. As can be seen, the identification in Case 2 agrees well with the original values. Tables 7 to 9 show, respectively, the correlation matrices of surge, sway, and yaw motion variables without additional signals, in which the constants μ_i ($i = 1,2,3$) are introduced

Table 6 Nondimensional hydrodynamic coefficients ($\times 10^{-5}$) of 20/20 deg zigzag maneuver

X-Coef.	Original	Estimate Case 1	Estimate Case 2	Y-Coef.	Original	Estimate Case 1	Estimate Case 2	N-Coef.	Original	Estimate Case 1	Estimate Case 2
$X'_{\dot{u}}$	−42	No estimate	No estimate	$Y'_{\dot{v}}$	−748	No estimate	No estimate	$N'_{\dot{v}}$	4.646	No estimate	No estimate
m'	798	No estimate	No estimate	$Y'_{\dot{r}}$	−9.354	No estimate	No estimate	$N'_{\dot{r}}$	−43.8	No estimate	No estimate
I'_z	39.2	No estimate	No estimate	Y'_v	−1,160	60,395	−1,160	N'_v	−264	−1,180	−264
x'_G	−2,300	No estimate	No estimate	Y'_r	−499	−874	−499	N'_r	−166	3,296	−166
X'_u	−184	−177	−184	Y'_{vvv}	−8,078	−39,071	−8,137	N'_{vvv}	1,636	2,118	1,537
X'_{uu}	−110	−117	−116	Y'_{vvr}	15,356	15,494	15,300	N'_{vvr}	−5,483	−7,210	−5,521
X'_{uuu}	−215	−215	−226	Y'_{vu}	−1,160	−62,717	−1,167	N'_{vu}	−264	652	−278
X'_{vv}	−899	−899	−903	Y'_{ru}	−499	−124	−503	N'_{ru}	−166	−3,627	−170
X'_{rr}	18	18	18	Y'_{δ}	278	278	278	N'_{δ}	−139	−139	−139
$X'_{\delta\delta}$	−95	−95	−95	$Y'_{\delta\delta\delta}$	−90	−90	−90	$N'_{\delta\delta\delta}$	45	45	45
$X'_{\delta\delta u}$	−190	−190	−190	$Y'_{\delta u}$	556	556	553	$N'_{\delta u}$	− 278	−278	−283
X'_{vr}	798	798	796	$Y'_{\delta uu}$	278	278	268	$N'_{\delta uu}$	−139	−140	−155
$X'_{v\delta}$	93	93	93	$Y'_{v\delta\delta}$	−4	−1.3	−1.6	$N'_{v\delta\delta}$	13	13	13
$X'_{v\delta u}$	93	93	92	$Y'_{vv\delta}$	1,190	1,177	1,161	$N'_{vv\delta}$	−489	−487	−506
				Y'_0	−4	− 3.5	−3.7	N'_0	3	3	1.3
				Y'_{0u}	−8	− 8.9	−8.5	N'_{0u}	6	6.2	9.1
				Y'_{0uu}	−4	− 3.3	−2.5	N'_{0uu}	3	3	12

Case 1: No ramp signal is added to the training samples and $C = 10^8$. Case 2: Ramp signal is added ($\lambda = 0.01$) and C decreases to 10^4.

Table 7 Correlation matrix of surge equation for 20/20 deg zigzag maneuver (Case 1)

	μ_1	a_1	a_2	a_3	a_4	a_5	a_6	a_7	a_8	a_9	a_{10}
μ_1	1.000	0.999	−0.971	0.921	−0.212	0.079	0.063	0.092	0.768	0.061	0.077
a_1		1.000	−0.959	0.903	−0.220	0.061	0.076	0.074	0.774	0.045	0.093
a_2			1.000	−0.986	0.203	−0.143	−0.029	−0.188	−0.705	−0.117	−0.014
a_3				1.000	−0.205	0.184	0.009	0.241	0.630	0.173	−0.053
a_4					1.000	0.724	−0.920	−0.155	−0.011	0.521	−0.522
a_5						1.000	−0.932	0.113	0.093	0.880	−0.786
a_6							1.000	0.049	−0.055	−0.773	0.727
a_7								1.000	−0.428	0.220	−0.150
a_8									1.000	−0.064	0.171
a_9										1.000	−0.948
a_{10}											1.000

Table 8 Correlation matrix of sway equation for 20/20 deg zigzag maneuver (Case 1)

	μ_2	b_{13}	b_{14}	b_{15}	b_1	b_2	b_7	b_3	b_8	b_4	b_{12}	b_{11}	b_9	b_5	b_6	b_{10}
μ_2	1.000	0.999	−0.910	0.953	−0.939	−0.967	0.901	0.506	0.512	−0.468	0.422	0.960	0.683	−0.115	−0.123	0.067
b_{13}		1.000	−0.914	0.952	−0.940	−0.958	0.895	0.512	0.518	−0.469	0.422	0.961	0.685	−0.129	−0.136	0.078
b_{14}			1.000	−0.865	0.906	0.842	−0.943	−0.795	−0.801	0.726	−0.664	−0.888	−0.768	0.130	0.135	−0.068
b_{15}				1.000	−0.984	−0.934	0.880	0.514	0.517	−0.508	0.479	0.893	0.746	−0.083	−0.091	0.044
b_1					1.000	0.901	−0.899	−0.629	−0.632	0.613	−0.578	−0.893	−0.835	0.090	0.096	−0.047
b_2						1.000	−0.913	−0.443	−0.448	0.447	−0.413	−0.915	−0.643	0.006	0.015	0.026
b_7							1.000	0.731	0.737	−0.750	0.712	0.864	0.755	0.000	−0.005	−0.027
b_3								1.000	0.996	−0.940	0.892	0.546	0.808	−0.081	−0.086	0.019
b_8									1.000	−0.937	0.887	0.552	0.798	−0.076	−0.081	0.015
b_4										1.000	−0.989	−0.499	−0.807	0.006	0.007	0.003
b_{12}											1.000	0.449	0.782	−0.042	−0.040	0.047
b_{11}												1.000	0.727	−0.107	−0.116	0.054
b_9													1.000	−0.034	−0.044	−0.004
b_5														1.000	0.997	−0.964
b_6															1.000	−0.959
b_{10}																1.000

Table 9 Correlation matrix of yaw equation for 20/20 deg zigzag maneuver (Case 1)

	μ_3	c_{13}	c_{14}	c_{15}	c_1	c_2	c_7	c_3	c_8	c_4	c_{12}	c_{11}	c_9	c_5	c_6	c_{10}
μ_3	1.000	−0.917	0.999	−0.870	0.910	0.855	−0.955	−0.793	−0.799	0.733	−0.673	−0.890	−0.771	0.116	0.122	−0.058
c_{13}		1.000	−0.914	0.952	−0.940	−0.958	0.895	0.512	0.518	−0.469	0.422	0.961	0.685	−0.129	−0.136	0.078
c_{14}			1.000	−0.865	0.906	0.842	−0.943	−0.795	−0.801	0.726	−0.664	−0.888	−0.768	0.130	0.135	−0.068
c_{15}				1.000	−0.984	−0.934	0.880	0.514	0.517	−0.508	0.479	0.893	0.746	−0.083	−0.091	0.044
c_1					1.000	0.901	−0.899	−0.629	−0.632	0.613	−0.578	−0.893	−0.835	0.090	0.096	−0.047
c_2						1.000	−0.913	−0.443	−0.448	0.447	−0.413	−0.915	−0.643	0.006	0.015	0.026
c_7							1.000	0.731	0.737	−0.750	0.712	0.864	0.755	0.000	−0.005	−0.027
c_3								1.000	0.996	−0.940	0.892	0.546	0.808	−0.081	−0.086	0.019
c_8									1.000	−0.937	0.887	0.552	0.798	−0.076	−0.081	0.015
c_4										1.000	−0.989	−0.499	−0.807	0.006	0.007	0.003
c_{12}											1.000	0.449	0.782	−0.042	−0.040	0.047
c_{11}												1.000	0.727	−0.107	−0.116	0.054
c_9													1.000	−0.034	−0.044	−0.004
c_5														1.000	0.997	−0.964
c_6															1.000	−0.959
c_{10}																1.000

Table 10 Correlation matrix of surge equation for 20/20 deg zigzag maneuver (Case 2)

	μ_1	a_1	a_2	a_3	a_4	a_5	a_6	a_7	a_8	a_9	a_{10}
μ_1	1.000	−0.531	0.588	−0.592	0.006	0.006	−0.029	−0.071	−0.441	0.100	−0.190
a_1		1.000	−0.959	0.903	−0.220	0.061	0.076	0.074	0.774	0.045	0.093
a_2			1.000	−0.986	0.203	−0.143	−0.029	−0.188	−0.705	−0.117	−0.014
a_3				1.000	−0.205	0.184	0.009	0.241	0.630	0.173	−0.053
a_4					1.000	0.724	−0.920	−0.155	−0.011	0.521	−0.522
a_5						1.000	−0.932	0.113	0.093	0.880	−0.786
a_6							1.000	0.049	−0.055	−0.773	0.727
a_7								1.000	−0.428	0.220	−0.150
a_8									1.000	−0.064	0.171
a_9										1.000	−0.948
a_{10}											1.000

Table 11 Correlation matrix of sway equation for 20/20 deg zigzag maneuver (Case 2)

	μ_2	b_{13}	b_{14}	b_{15}	b_1	b_2	b_7	b_3	b_8	b_4	b_{12}	b_{11}	b_9	b_5	b_6	b_{10}
μ_2	1.000	0.636	−0.605	0.580	−0.582	−0.576	0.570	0.367	0.369	−0.352	0.359	0.602	0.417	−0.645	−0.641	0.640
b_{13}		1.000	−0.914	0.952	−0.940	−0.958	0.895	0.512	0.518	−0.469	0.422	0.961	0.685	−0.129	−0.136	0.078
b_{14}			1.000	−0.865	0.906	0.842	−0.943	−0.795	−0.801	0.726	−0.664	−0.888	−0.768	0.130	0.135	−0.068
b_{15}				1.000	−0.984	−0.934	0.880	0.514	0.517	−0.508	0.479	0.893	0.746	−0.083	−0.091	0.044
b_1					1.000	0.901	−0.899	−0.629	−0.632	0.613	−0.578	−0.893	−0.835	0.090	0.096	−0.047
b_2						1.000	−0.913	−0.443	−0.448	0.447	−0.413	−0.915	−0.643	0.006	0.015	0.026
b_7							1.000	0.731	0.737	−0.750	0.712	0.864	0.755	0.000	−0.005	−0.027
b_3								1.000	0.996	−0.940	0.892	0.546	0.808	−0.081	−0.086	0.019
b_8									1.000	−0.937	0.887	0.552	0.798	−0.076	−0.081	0.015
b_4										1.000	−0.989	−0.499	−0.807	0.006	0.007	0.003
b_{12}											1.000	0.449	0.782	−0.042	−0.040	0.047
b_{11}												1.000	0.727	−0.107	−0.116	0.054
b_9													1.000	−0.034	−0.044	−0.004
b_5														1.000	0.997	−0.964
b_6															1.000	−0.959
b_{10}																1.000

Table 12 Correlation matrix of yaw equation for 20/20 deg zlgzag maneuver (Case 2)

	μ_3	c_{13}	c_{14}	c_{15}	c_1	c_2	c_7	c_3	c_8	c_4	c_{12}	c_{11}	c_9	c_5	c_6	c_{10}
μ_3	1.000	0.136	−0.155	0.095	−0.106	−0.082	0.116	0.123	0.121	−0.130	0.170	0.119	0.068	−0.747	−0.737	0.775
c_{13}		1.000	−0.914	0.952	−0.940	−0.958	0.895	0.512	0.518	−0.469	0.422	0.961	0.685	−0.129	−0.136	0.078
c_{14}			1.000	−0.865	0.906	0.842	−0.943	−0.795	−0.801	0.726	−0.664	−0.888	−0.768	0.130	0.135	−0.068
c_{15}				1.000	−0.984	−0.934	0.880	0.514	0.517	−0.508	0.479	0.893	0.746	−0.083	−0.091	0.044
c_1					1.000	0.901	−0.899	−0.629	−0.632	0.613	−0.578	−0.893	−0.835	0.090	0.096	−0.047
c_2						1.000	−0.913	−0.443	−0.448	0.447	−0.413	−0.915	−0.643	0.006	0.015	0.026
c_7							1.000	0.731	0.737	−0.750	0.712	0.864	0.755	0.000	−0.005	−0.027
c_3								1.000	0.996	−0.940	0.892	0.546	0.808	−0.081	−0.086	0.019
c_8									1.000	−0.937	0.887	0.552	0.798	−0.076	−0.081	0.015
c_4										1.000	−0.989	−0.499	−0.807	0.006	0.007	0.003
c_{12}											1.000	0.449	0.782	−0.042	−0.040	0.047
c_{11}												1.000	0.727	−0.107	−0.116	0.054
c_9													1.000	−0.034	−0.044	−0.004
c_5														1.000	0.997	−0.964
c_6															1.000	−0.959
c_{10}																1.000

Table 13 Condition numbers

	Case 1	Case 2
Surge	4.3×10^{8}	7.8×10^{6}
Sway	7.4×10^{15}	6.6×10^{8}
Yaw	1.8×10^{20}	6.6×10^{8}

correspondingly to the unit elements in ***A, B, C*** (equations 20). Tables 10 to 12 show, respectively, the correlation matrices of surge, sway, and yaw motion variables after the additional signal is attached. The corresponding condition numbers of the three correlation matrices are shown in Table 13. It can be seen from these tables, without additional signals, strong correlation and large condition numbers result in the high degree of multicollinearity, especially for the sway and yaw motion and for the linear derivatives, and the corresponding condition numbers decrease after modification.

The approximation errors by using SVM for surge speed, sway speed, and yaw rate are given in Fig. 1. Figures 2 and 3 show the comparison of the predicted motions using the better identified hydrodynamic coefficient with the simulated motions. As can be seen, the results of learning and prediction are satisfactory.

4.3. Analysis of predictive ability

As an artificial intelligence learning method, no matter neural network–based or SVM-based method, it is valuable only if it has good predictive ability. A well-trained SVM regression model should be able to predict maneuvers, which are different from the training maneuvers. As mentioned before, the SVM has the satisfactory predictive ability because its cost function contains

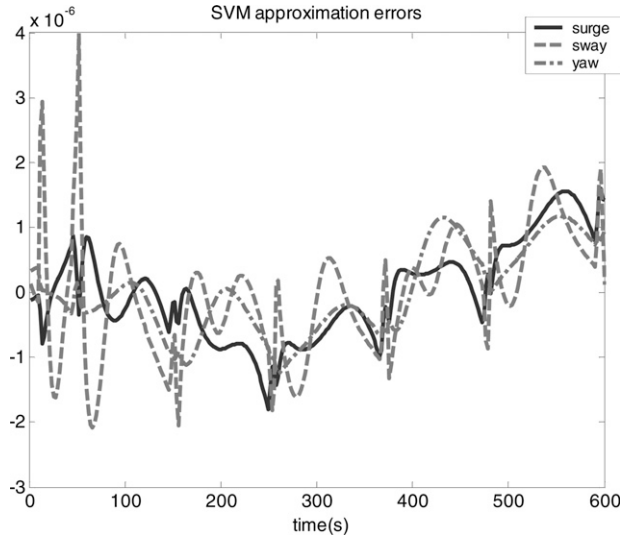

Fig. 1 Approximation errors by using support vector machines (SVM) for surge speed, sway speed, and yaw rate

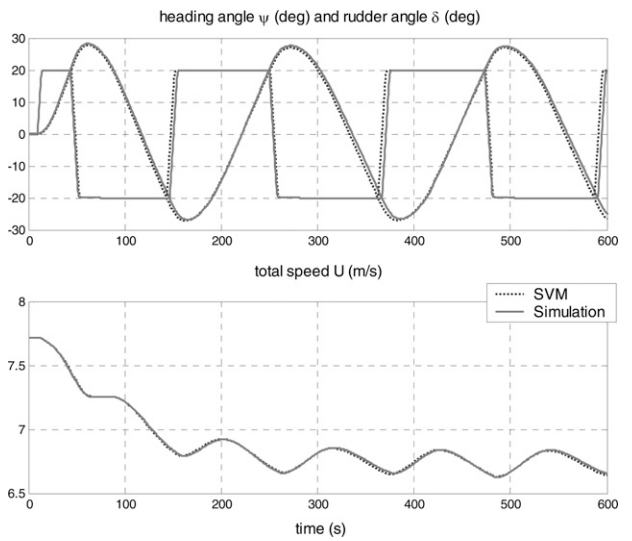

Fig. 2 Predicted heading and ship speed of 20/20 deg zigzag maneuver

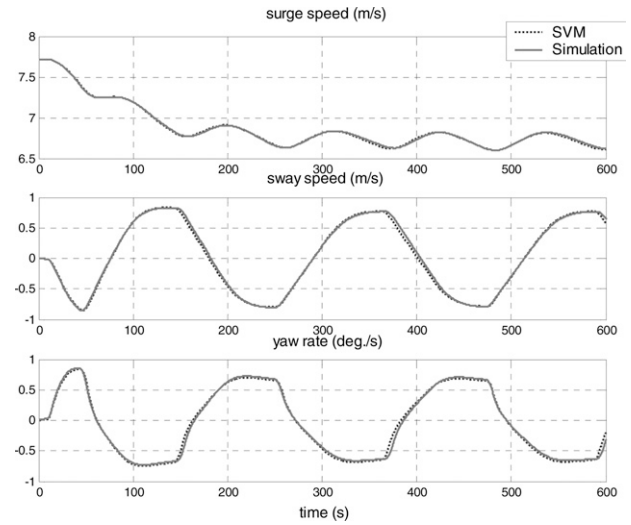

Fig. 3 Predicted surge speed, sway speed, and yaw rate of 20/20 deg zigzag maneuver, respectively

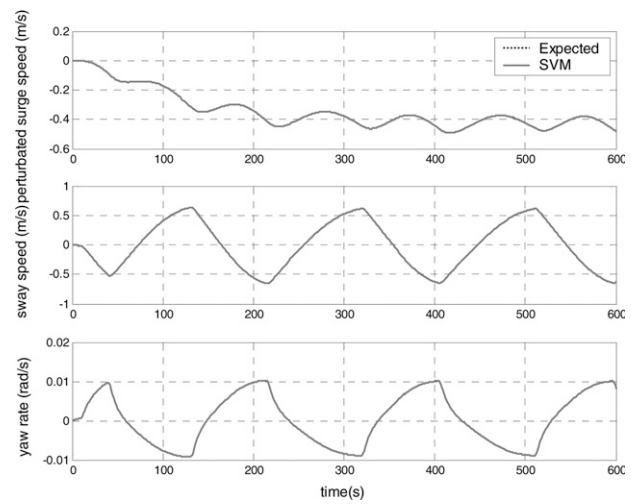

Fig. 4 Prediction of 10/10 deg zigzag maneuver

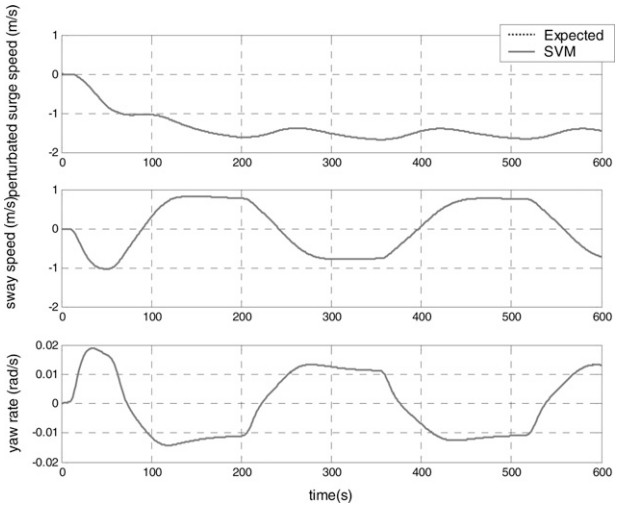

Fig. 5 Prediction of 35/35 deg zigzag maneuver

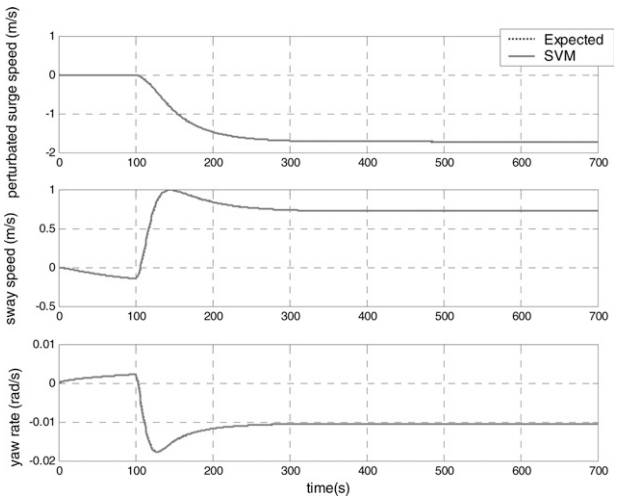

Fig. 6 Prediction of 35 deg starboard turning

not only approximation errors but also VC dimension. To check this ability, three maneuvers, 10/10 deg, 35/35 deg zigzag, and 35 deg turning at an approach speed of 15 knots (7.717 m/s), are simulated to obtain the reference data. Three hundred support vectors, 300 Lagrangian factors, and one bias obtained in 20/20 deg zigzag maneuver are used while predicting 600 data samples for zigzag maneuvers and 700 for turning. The results are shown in Figs. 4 to 6.

As can be seen from the figures, good agreements between the predicted and simulated velocities are obtained. The good predictive ability of the trained SVM is confirmed.

5. Conclusions

In this paper, a novel method of system identification derived from statistical learning theory, support vector machines, is applied to identify the hydrodynamic coefficients in nonlinear maneuvering models for surface ships. Different from the iterative algorithms used in traditional identification techniques, this kind of artificial intelligence method can satisfactorily diminish the simultaneous drift and multicollinearity effects. It requires no initial estimation of parameters. Not only is the nonlinear mapping underlying the maneuvering motion well approximated, but also the hydrodynamic coefficients are successfully obtained from the structure of SVM by using a linear kernel function. Moreover, the trained SVM using simulations of a 20/20 deg zigzag maneuver shows good ability to predict other maneuvers. The preliminary results of identification and simulation have demonstrated the validity of the method. More work is needed to improve and verify this method to make it a powerful and successful one. First, further research is required to investigate the related techniques, such as effectively choosing the parameters of SVM, including the kernel, the regularization parameter C, and the insensitivity factor ε. Second, the on-line learning ability and the efficiency of large sample training in SVM require further research, which is valuable in real-time prediction and steering. Third, further work is to be focused on verification of the proposed method by using the data from sea trials or free-running model tests. Smoothing the measured data can be conducted, either by using SVM or other filter techniques. Sometimes, estimating for the unmeasurable variables is necessary, for example, by using the extended Kalman filter (EKF). Then SVM can be applied to the parameter identification of the processed data. The hydrodynamic coefficients can be obtained from the expansion of the kernel function.

Acknowledgments

This work is financially supported by the Special Research Fund for the Doctoral Program of Higher Education of China (No. 20050248037) and the National Natural Science Foundation of China (No. 50779033).

References

Abkowitz, M.A. 1964 *Lectures on Ship Hydrodynamics Steering and Manoeuvrability*, Hydro- and Aerodynamics Laboratory, Report No. Hy-5, Denmark.

Abkowitz, M.A. 1980 Measurement of hydrodynamic characteristic from ship maneuvering trials by system identification, *Transactions of the Society of Naval Architects and Marine Engineers*, **88,** 283–318.

Åstrom, K.J., and Källström, C.G. 1976 Identification of ship steering dynamics, *Automatica*, **12,** 9–22.

Bhattacharyya, S.K., and Haddara, M.R. 2006 Parameter identification for nonlinear ship manoeuvring, Journal of Ship Research, **50,** 3, 197–207.

Blanz, V., Schölkopf, B., Bülthoff, H., Burges, C., Vapnik, N., and Vetter, T. 1996 Comparison of view-based object recognition algorithms using realistic 3D models, *Proceedings*, 1996 International Conference on Artificial Neural Networks, Lecture Notes In Computer Science, July, London, UK, **1112,** 251–256.

Chislett, M.S., and Strom-Tejsen, J. 1965 Planar motion mechanism tests and full-scale steering and maneuvering predictions for a Mariner Class Vessel, *International Shipbuilding Progress*, **129,** 12, 201–224.

Drezet, P.M.L., and Harrison, R.F. 1998 Support vector machines for system identification, *Proceedings*, UKACC International Conference on CONTROL'98, September, University of Wales, Swansea, UK, 688–692.

Fossen, T.I. 1994 *Guidance and Control of Ocean Vehicles*, John Wiley and Sons, New York.

Goethals, I., Pelckmans, K., Suykens, J.A.K., and De Moor, B. 2005 Identification of MIMO Hammerstein models using least squares support vector machines, *Automatica*, **41,** 1263–1272.

GRETTON, A., DOUCET, A., HERBRICH, R., RAYNER, P.J.W., AND SCHÖLKOPF, B. 2001 Support vector regression for black-box system identification, *Proceedings*, 11th IEEE Signal Processing Workshop on Statistical Signal Processing, August, Singapore, 341–344.

HADDARA, M.R., AND WANG, Y. 1999 Parametric identification of maneuvering models for ships, *International Shipbuilding Progress*, **46,** 445, 5–27.

HAYES, M.N. 1971 *Parameters Identification of Nonlinear Stochastic Systems Applied to Ocean Vehicle Dynamics*, Ph.D. thesis, Massachusetts Institute of Technology, Cambridge, MA.

HWANG, W.Y. 1980 *Application of System Identification to Ship Maneuvering*, Ph.D. thesis, Massachusetts Institute of Technology, Cambridge, MA.

HWANG, W.Y. 1982 Cancellation effect and parameter identifiability of ship steering dynamics, *International Shipbuilding Progress*, **26,** 332, 90–120.

IMO. 1993 *Interim Standards for Ship Manoeuvrability*, Resolution A.751 (18), International Maritime Organization.

IMO. 2002 *Standards for Ship Manoeuvrability*, Resolution MSC.137(76), International Maritime Organization.

ITTC. 2005 Report of Maneuvering Committee, *Proceedings*, 24th International Towing Tank Conference, September, Edinburgh, UK, 1, 138–146.

IVAKHNENKO, A.G., AND MULLER, J.A. 1995 Present state and new problems of further GMDH development, *Systems Analysis Modeling Simulation*, **20,** 1–2, 3–16.

KÄLLSTRÖM, C.G., AND ÅSTRÖM, K.J. 1981 Experiences of system identification applied to ship steering, *Automatica*, **17,** 187–198.

KEERTHI, S.S., AND SHEVADE, S.K. 2003 SMO algorithm for least squares SVM, *Proceedings*, International Joint Conference on Neural Networks, July, Portland, OR, vol. 3, 2088–2093.

LASKOV, P. 2002 Feasible direction decomposition algorithms for training support vector machines, *Machine Learning*, **46,** 1, 315–349.

LIN, C.F., AND WANG, S.D. 2002 Fuzzy support vector machines, *IEEE Transactions on Neural Networks*, **13,** 2, 464–471.

MAHFOUZ, A.B., AND HADDARA, M.R. 2003 Effects of the damping and excitation on the identification of the hydrodynamic parameters for an underwater robotic vehicle, *Ocean Engineering*, **30,** 1005–1025.

MASSY, W.F. 1965 Principal components regression in exploratory statistical research, *Journal of the American Statistical Association*, **60,** 309, 234–256.

PLATT, J.C. 1998 Fast training of support vector machines using sequential minimal optimization, in Schölkopf, B., Burges, C. J. C., and Smola, A. J., editors, *Advances in Kernel Methods—Support Vector Learning*, MIT Press, Cambridge, MA, 185–208.

RHEE, K.P., LEE, S.Y., AND SUNG, Y.J. 1998 Estimation of manoeuvring coefficients from PMM test by genetic algorithm, *Proceedings*, International Symposium and Workshop on Force Acting on a Manoeuvring Vessel, September, Val de Reuil, France, 77–87.

SCHÖLKOPF, B., SMOLA, A.J., WILLIAMSON, R.C., AND BARTLETT, P.L. 2000 New support vector algorithms, *Neural Computation*, **12,** 1207–1245.

SELVAM, R.P., BHATTACHARYYA, S.K., AND HADDARA, M.R. 2005 A frequency domain system identification method for linear ship manoeuvring, *International Shipbuilding Progress*, **52,** 1, 5–27.

SUYKENS, J.A.K., AND VANDEWALLE, J. 1999 Least squares support vector machines classifiers, *Neural Processing Letters*, **9,** 293–300.

SYED, N.A., LIU, H., AND SUNG, K.K. 1999 Incremental learning with support vector machines, *Proceedings*, International Joint Conference on Artificial Intelligence (IJCAI-99), July, Stockholm, Sweden.

VAPNIK, V.N. 1998 *Statistical Learning Theory*, John Wiley and Sons, New York.

VAPNIK, V.N. 1999 An overview of statistical learning theory, *IEEE Transactions on Neural Networks*, **10,** 5, 988–999.

VAPNIK, V.N. 2005 Universal learning technology: support vector machines, *NEC Journal of Advanced Technology*, **2,** 2, 137–144.

WOLD, S., et al. 1984 The collinearity problem in linear regression, the Partial Least Squares (PLS) approach to generalized inverses, *SIAM Journal on Scientific and Statistical Computing*, **5,** 3, 735–743.

YEON, S.M., YEO, D.J., AND RHEE, K.P. 2006 Optimal input design for the identification of low-speed manoeuvring mathematical model, *Proceedings*, International Conference on Marine Simulation and Ship Manoeuvrability (MARSIM'06), June, Terschelling, Netherlands.

YOON, H.K., AND RHEE, K.P. 2003 Identification of hydrodynamic coefficients in ship maneuvering equations of motion by estimation-before-modeling technique, *Ocean Engineering*, **30,** 2379–2404.

ZHOU, W.W. 1989 Identification of a class of nonlinear state-space models using RPE techniques, *IEEE Transactions on Automatic Control*, **34,** 3, 312–316.